Journal of Fluorescence, Vol. 2, No. 3, 1992

The Use of the Isotropic Orientation Factor in Fluorescence Resonance Energy Transfer (FRET) Studies of the Actin Filament

Richard Censullo,[1,2] James C. Martin,[1] and Herbert C. Cheung[1,3]

Received July 10, 1992; revised October 21, 1992; accepted October 22, 1992

A Dale–Eisinger style analysis (R. E. Dale *et al., Biophys. J.* **26,** 161, 1979) is used to produce three-dimensional plots that display the limits on the average orientation factor $\langle\kappa^2\rangle$ that is required to calculate molecular distances in F-actin from fluorescence resonance energy transfer measurements. Maxima and minima plots are generated for the transfer of energy from a donor to a single acceptor and for transfer to multiple acceptors that are related by F-actin helical symmetry. The analysis is performed in terms of dipole cone half-angles rather than depolarization factors, in order to facilitate the modeling of the multiple acceptor problem. Calculations are carried out under the restrictive condition of a single electric dipole moment per fluorophore. In addition, both surface and volume averaging of the donor and acceptor dipoles are considered. Comparisons between the plots show that for the multiple acceptor cases with F-actin symmetry, there is a great reduction in the range for maxima and minima limits on $\langle\kappa^2\rangle$. The calculations also suggest guidelines for the choice of fluorescence label that will result in an average orientation factor occurring within acceptable limits, i.e., inside the limits for which $\langle\kappa^2\rangle = 2/3$ may be employed. Thus, without having detailed knowledge of the mean donor or acceptor dipole relative orientations, the use of $\langle\kappa^2\rangle = 2/3$ in radial coordinate studies of F-actin is more than reasonable and is fairly assured of being correct.

KEY WORDS: Isotropic orientation factor; fluorescence resonance energy transfer; actin filament.

INTRODUCTION

Molecular Distances and FRET

Fluorescence resonance energy transfer (FRET) between donor and acceptor fluorophores has been widely used to determine molecular distances between specific sites in a variety of proteins [1]. This method offers an experimental approach to determination of molecular distances in the range 10–80 Å and, because of the inverse sixth power dependence of the transfer efficiency on the donor–acceptor distance [2], is particularly sensitive to global structural changes. From the observed average efficiency of energy transfer $\langle E\rangle$, the distance r between donor and acceptor may be calculated from

$$\langle E\rangle = R_o^6/(R_o^6 + r^6) \qquad (1)$$

R_o is the Förster critical distance at which the transfer efficiency is 50% and is given (in Å) by $R_o = 9.79 \times 10^3\ (n^{-4}QJ\kappa^2)^{1/6}$, where n is the refractive index of the

[1] Department of Physics, University of Alabama at Birmingham, University Station, Birmingham, Alabama 35294.
[2] To whom correspondence should be addressed at Department of Physics, University of Alabama at Birmingham, Birmingham, Alabama 35294-1170.
[3] Department of Biochemistry, University of Alabama at Birmingham, University Station, Birmingham, Alabama 35294.

1053-0509/92/0900-0141$06.50/0

medium, Q the donor quantum yield, J the spectral overlap integral between the donor emission spectrum and the acceptor absorption spectrum, and κ^2 the orientation factor of the transition dipole moments. The efficacy of this technique in providing accurate distances possess an inherent limitation due to the uncertainty in the value for the orientation factor. In the limit of isotropic dynamic averaging of the motions of the transition dipoles, κ^2 is 2/3. If this value is used, as is frequently the case, one obtains an apparent distance $r_{2/3}$ which is related to the actual distance r by

$$r = (1.5\kappa^2)^{1/6} r_{2/3} \tag{2}$$

Since the range for κ^2 is 0–4, the actual value of r can be in the range of $(0–1.35)r_{2/3}$. This uncertainty does not in itself diminish the power of FRET to provide a measure of molecular distances. Several approaches [3–5] have been proposed to deal with the κ^2 problem and to estimate the error resulting from using the value of 2/3 in calculating molecular distances from Eq. (1). The general consensus is that the most cautious approach to this problem is to establish the maximum and minimum values of the average orientation factor $\langle\kappa^2\rangle$, based on observed depolarization parameters of both donor and acceptor. This approach yields the lower and upper bounds of r and provides an indication of the range of possible values to be expected. This range has been experimentally shown to be narrow for certain systems and also can be expected to be reduced for fluorophores that exhibit mixed polarization [4].

If the transfer of resonance energy is between a donor–acceptor system located on adjacent monomeric subunits in a polymer that is helically symmetric, then the observed transfer efficiency can be related to the distance of the fluorophores from the theoretical axis of the helix. This approach has been used to determine the radial coordinates of several residues of the helical F-actin filament [6–8]. In these studies, κ^2 was generally assumed to be 2/3. While the likely range of κ^2 for F-actin may be considerably smaller than 0–4 because of the symmetrical arrangement of the donor and acceptor positions along the helix and transfer to multiple acceptors, it is not immediately clear to what extent the use of the value 2/3 is a good approximation. In the present work, we have generated plots for the maxima and minima of κ^2 for transfer to multiple acceptors that are related by the actin helix symmetry. In addition, we have used both surface and volume averaging of the donor and acceptor dipoles in order to investigate the effect of these models on the orientation factor. For the multiple acceptor cases with actin symmetry, the range for maxima and minima limits on $\langle\kappa^2\rangle$ is shown to be greatly reduced. Physically, this corresponds to the ability to use fluorophores with smaller cone half-angles in these multiple acceptor arrangements and still justifiably employ the $\langle\kappa^2\rangle = 2/3$ approximation.

The Orientation Factor

We first summarize the expressions for the orientation factor (Fig. 1). The two equivalent formulae for the static orientation factor, in which the dipoles are assumed to be immobile over the duration of energy transfer, are as follows [5]:

$$\kappa^2 = (\cos\theta_T - 3\cos\theta_D \cos\theta_A)^2 \tag{3}$$

$$\kappa^2 = (\sin\theta_D \sin\theta_A \cos\phi - 2\cos\theta_D \cos\theta_A)^2 \tag{4}$$

When either the donor or the acceptor dipoles (or both) have some freedom of movement over the time interval in which energy transfer takes place, the dynamically averaged orientation factor is given by Eq. (5):

$$\begin{aligned}\langle\kappa^2\rangle = {} & \kappa^{x2}\langle d_D^x\rangle\langle d_A^x\rangle + 1/3(1 - \langle d_D^x\rangle) \\ & + 1/3(1 - \langle d_A^x\rangle) + \cos^2\Theta_D\langle d_D^x\rangle(1 - \langle d_A^x\rangle) \\ & + \cos^2\Theta_A\langle d_A^x\rangle(1 - \langle d_D^x\rangle)\end{aligned} \tag{5}$$

where

$$\kappa^{x2} = (\sin\Theta_D \sin\Theta_A \cos\phi - 2\cos\Theta_D \cos\Theta_A)^2 \tag{6}$$

and

$$\langle d_D^x\rangle = 3/2\,\langle\cos^2\psi_D\rangle - 1/2 \tag{7}$$

$$\langle d_D^x\rangle = 3/2\,\langle\cos^2\psi_A\rangle - 1/2 \tag{8}$$

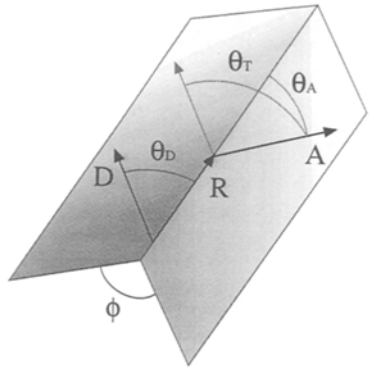

Fig. 1. Spatial relationships between donor and acceptor dipoles. θ_D is the angle between the donor dipole and **R** (the vector from the donor to the acceptor). θ_A is the angle between the acceptor dipole and **R**. θ_T is the angle between donor and acceptor dipoles, and ϕ represents the angle between the planes defined separately by the donor and acceptor each with the vector **R**.

In Eqs. (5)–(8), κ^{x2} stands for the axial orientation factor, which is defined for the mean orientations of the donor D and acceptor A. (The mean orientations can be expressed as D^x and A^x.) The parameters $\langle d^x{}_D \rangle$ and $\langle d^x{}_A \rangle$ stand for the donor and acceptor axial depolarization factors, respectively. Each of these depolarization factors in turn depends on the average cone half-angle for that dipole, either ψ_D or ψ_A (Fig. 2). The cone half-angle ψ is the angle from a theoretical central vector within the cone (D^x or A^x) to a vector that represents the maximum extent of the dipole and lies along the outside surface of the cone. The angles Θ and Φ in Eq. (6) are the counterparts to θ and ϕ in Eq. (4), simply measured from the theoretical central vector (mean orientation of the dipole) within the cone. In Fig. 1, the dynamically averaged $\langle \kappa^2 \rangle$ would be represented by having D^x and A^x replace D and A, each surrounded by an appropriate axially symmetric cone distribution (Fig. 2 and following section).

The maxima and minima of the dynamically averaged orientation factor cannot be obtained by merely aligning the dipoles in-line parallel or mutually perpendicular (respectively), as in the static case [Eqs. (3) and (4)]. A complete analytic solution for the extrema under dynamically averaged conditions is very difficult, and the problem is more suitable for a computer-based search [5].

Errors Produced by the Use of $\langle \kappa^2 \rangle = 2/3$

The correlation of an actual value for $\langle \kappa^2 \rangle$ with the error produced on r due to the general use of $\langle \kappa^2 \rangle = 2/3$ can be seen by rewriting Eq. (2):

$$\kappa^2 = 2/3\ (r/r_{2/3})^6 \qquad (9)$$

Therefore if the desired goal is to have $r_{2/3}$ be no less than 20% smaller than r (a ratio of $r/r_{2/3} = 1/0.8$), then Eq. (9) shows that κ^2 can be no greater than 2.54. Similarly, for $r_{2/3}$ to be no more than 20% greater than r (a ratio of $r/r_{2/3} = 1/1.2$), κ^2 can be no less than 0.22. Correspondingly, an underestimation or overestimation of the distance r by 10% yields limits of $\kappa^2 = 1.25$ and $\kappa^2 = 0.38$, respectively.

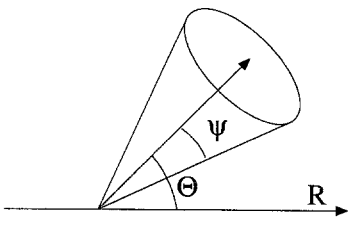

Fig. 2 Cone half-angle of a dipole. The angle ψ represents the maximum extent of the angle between the dipole and a theoretical central vector within the cone (i.e., the mean orientation or symmetry axis). The angle between this central vector (either D^x or A^x) and the **R** vector (from Fig. 1) is given by Θ.

Surface and Volume Averaging

In the equations for the depolarization factors [Eqs. (7) and (8)] the value of the average $\cos^2\psi$ term is strongly dependent on the model that is assumed for the orientational freedom of the dipole. Surface averaging (Fig. 3a) refers to the situation in which the dipole precesses around the outside surface of a cone during the time that energy transfer takes place. In this case, the tip of the vector that represents the dipole describes a circle. Note that the angle between the dipole and the theoretical center vector of the cone is constant during energy transfer and is equal to ψ. Thus, the average term $\langle \cos^2\psi \rangle$ is simply equal to $\cos^2\psi$.

$$\langle \cos^2\psi \rangle_{surf} = \cos^2\psi \qquad (10)$$

The situation for volume averaging assumes that, during the time of energy transfer, the vector that represents the dipole can be found anywhere with equal probability within the cone of half-angle ψ (Fig. 3b). Here the tip

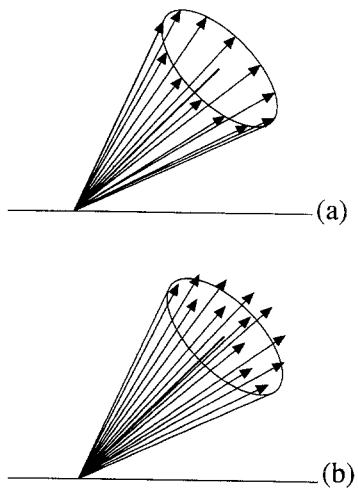

Fig. 3. Dipole surface and volume averaging. (a) Surface averaging. This shows a dipole rotating around a central axis in such a way that the tip of the vector is always found on a fixed circle. Correspondingly, the body of the vector is always found to lay on the surface of a cone. (b) Volume averaging. In this case the tip of the vector is found anywhere on a spherical section capping the cone, and the body of the vector can be found either on the surface or in the interior of the cone. In both a and b, the cone half-angle is represented in the same manner as in Fig. 2.

of the dipole vector sweeps out an element of surface area on a sphere during energy transfer. At any particular moment, the angle between the dipole and the theoretical central vector will have a value between 0 and ψ. This means that the $\langle\cos^2\psi\rangle$ term must be averaged appropriately [9] and is not simply equal to $\cos^2\psi$.

$$\langle\cos^2\psi\rangle_{vol} = (1 + \cos\psi + \cos^2\psi)/3 \qquad (11)$$

The conditions under which Eq. (5) will yield the exact isotropic orientation factor 2/3 (i.e., when both donor and acceptor depolarization factors $\langle d^x\rangle$ fall to zero) can be obtained from any combination of the following ψ for both donors and acceptors: $\psi = \pi/2$ or π for volume averaging, and $\psi = 54.7$ or $125.3°$ for surface averaging. Figure 4 shows the effect that the choice of model for the motion of dipole moments within a cone has on the average cone half-angle $\langle\cos^2\psi\rangle$ and the axial depolarization factor $\langle d^x\rangle$ [Eqs. (7), (8)].

Energy Transfer in the Actin Filament

It was first shown by Taylor *et al.* [6] that energy transfer between donor and acceptor pairs located at chemically equivalent sites along the helical actin filament provided sufficient information to calculate the radial coordinate r_a of the site. Experimentally, one sample of monomeric G-actin is labeled with a donor probe at a specific residue and another sample is labeled with an acceptor probe at the same residue. These two samples are then mixed and the labeled G-actin is allowed to polymerize to form helical filaments. Depending on the ratio of the two populations of labeled monomeric actin used in the polymerization, a given donor-labeled subunit in the polymer may be surrounded by one or more acceptor-labeled subunits [8]. Figure 5 shows the geometry of the filament in which actin subunit 0 is labeled with a donor fluorophore and the adjacent subunits are labeled with the acceptor. Excitation energy is assumed to transfer from subunit 0 to subunits $+1$, $+2$, -1, and -2 if these subunits actually contain the acceptor, and the transfer is assumed not to extend further than the ± 2 subunits [6, 8].

Even though they are attached at chemically equivalent residues, the donor and acceptor labels are assumed to be chemically different. Therefore, there is no correlation between the cone half-angles ψ_D and ψ_A or between angle Θ_D and angle Θ_A. Note, however, that the cone half-angles of all four acceptors are identical ($\psi_{A+1} = \psi_{A+2} = \psi_{A-1} = \psi_{A-2}$). Also note that from the angle Θ_{A+1}, which is associated with the mean orientation of the acceptor attached to subunit $+1$, the other acceptor Θ angles for subunits $+2$, -1, and -2 can be generated using the helical symmetry of F-actin. A full discussion of the symmetry relationships for multiple acceptors within F-actin is given in the Appendix.

METHODS

Calculations

The calculation of minima and maxima data for the three-dimensional plots was carried out using the Mathematica software package (Wolfram Research) on a SPARCstation 2 computer (Sun Microsystems). The average time needed to generate the data for a single plot was approximately 30 h. The Mathematica software package, an (Apple) Macintosh IIcx computer, and a Laserwriter II printer were used to produce the plots from the calculated data.

The Maxima and Minima Plots

Figures 6–8 show the three-dimensional plots of the maxima and minima for the dynamically averaged orientation factor $\langle\kappa^2\rangle$ vs the cone half-angle of the donor ψ_D and the cone half-angle of the acceptor ψ_A. These plots correspond to transfer to a single acceptor, transfer to four acceptors in F-actin, and transfer to the two nearest acceptors in F-actin, respectively. For the ease of comparison, each figure shows the plots that are obtained from traditional surface averaging displayed next to the plots obtained from volume averaging.

These figures follow the convention set by Dale *et al.* [5] with regard to the shading that indicates the amount of error generated by the use of $\langle\kappa^2\rangle = 2/3$. The unshaded (white) regions of the plot indicate that, for those particular combinations of cone half-angles, the possible maximum (or minimum) value for $\langle\kappa^2\rangle$ is such that the use of $\langle\kappa^2\rangle = 2/3$ would result in a calculated distance $r_{2/3}$ that is within $\pm 10\%$ of the actual distance r [Eq. (9)]. A light gray region of the plot corresponds to regions where the use of $\langle\kappa^2\rangle = 2/3$ would result in a 10–20% error in r, and a darkly shaded region indicates that the error would exceed 20%. Thus darkly shaded regions represent what is generally considered as being outside the realm of acceptability for the calculation of donor–acceptor distances.

For each particular combination of the parameters ψ_D and ψ_A, all possible orientations for the cone central vector are tested, e.g., Θ_D, Θ_A, and Φ [Eq. (5)]. From all of these orientations, thousands of possible values for

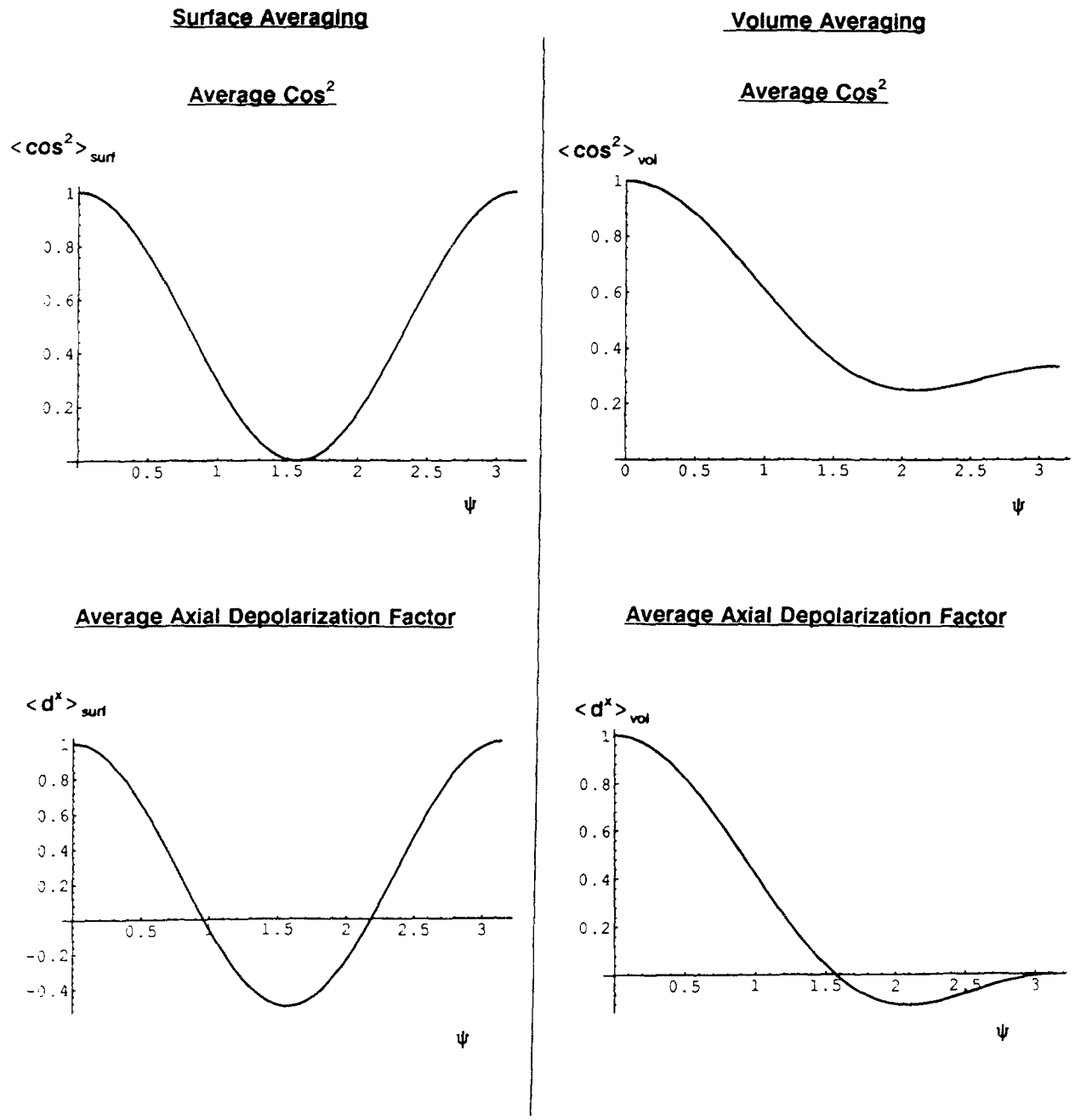

Fig. 4. Model dependence of the average $\cos^2$ and the average axial depolarization factor. The effect of dipole surface or volume averaging on these two quantitites is shown as a function of the cone half-angle ψ (given in radians); see Eqs. (7), (8), (10), and (11).

$\langle\kappa^2\rangle$ are generated for an individual ψ_D and ψ_A. The maximum and minimum average orientation factor can then be generated for the entire set of ψ_D and ψ_A. Thus, any small grid area in Figs. 6–8 represents the most extreme value for $\langle\kappa^2\rangle$ at those given cone half-angles, even though this value may occur as infrequently as only once, i.e., for a single orientation (Θ_D, Θ_A, Φ). The usefulness of these "worst-case" maxima and minima plots is that it can be stated with certainty that the application of $\langle\kappa^2\rangle = 2/3$ will always result in distance

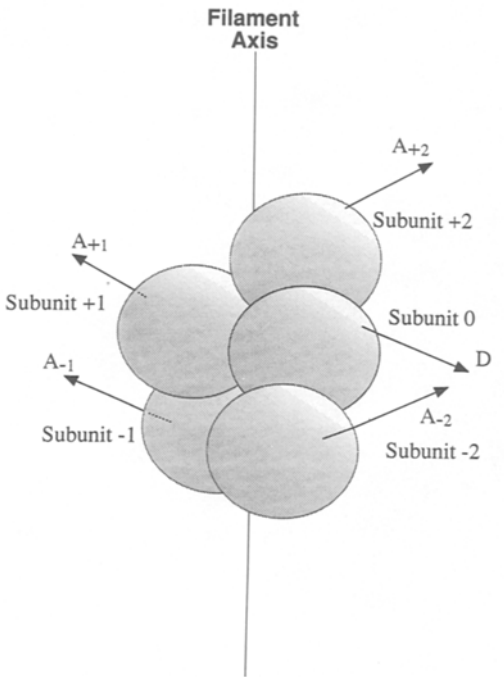

Fig. 5. Geometry of the labeled actin filament. A donor chromophore, depicted by vector **D**, labels actin unit 0. Four identical acceptor labels: $\mathbf{A}_{+1}$, $\mathbf{A}_{+2}$, $\mathbf{A}_{-1}$, and $\mathbf{A}_{-2}$ are shown attached to their respective actin units. The acceptor vectors are all rotationally related by the underlying F-actin symmetry. The spatial orientation of the donor dipole has no relation to the orientation of the acceptors, although the donor and acceptors each label identical residues within their respective subunits. (The vectors depicted here can be considered to be either donor and acceptor dipoles of cone half-angle 0°, or the axis of symmetry of the individual dipole distributions.)

calculations that have 10% or less error for unshaded areas and 20% or less error for lightly shaded areas. For these areas, there are no combinations of angular orientations for the cone central vectors that can produce unacceptable $\langle\kappa^2\rangle$ values.

RESULTS

Transfer from a Single Donor to a Single Acceptor/ General Case

The shapes of the maxima and minima plots for transfer between a single donor and a single acceptor differ strongly (Fig. 6). The regions of acceptability and unacceptability also differ. When surface averaging is applied, there are more combinations of cone half-angles that produce poor average orientation factors. On the other hand, volume averaging yields relatively good behavior for the plots, as a large fraction of the surface falls within the error range of $\pm 10\%$. As may be expected for volume averaging, both $\langle\kappa^2\rangle_{max}$ and $\langle\kappa^2\rangle_{min}$ converge to 2/3 as both ψ_D and ψ_A approach π (complete isotropy). Thus for volume averaging, concern over the use of the isotropic orientation factor occurs only when both donor and acceptor ψ are less than 60°.

Transfer from One Donor to Four Acceptors/Actin Filament

Due to the use of the cone half-angle parameter, simple spatial symmetry relationships between the helically related multiple acceptor dipoles can be derived (Appendix). This method allows the plots shown in Figs. 7 and 8 to be produced in a straightforward manner, analogous to the single donor–acceptor pair (Fig. 6).

Figure 7 shows the situation in which a donor transfers excitation energy to four acceptors concurrently. This case is investigated for transfer between monomeric subunits in the actin filament (Fig. 5) at radial coordinate $r_a = 25$ Å. At this radial coordinate the intermonomer distance between the donor and each of the four acceptors is the same [8]. The overall shapes of these plots are similar to those for the single donor–single acceptor case (Fig. 6), but the range of $\langle\kappa^2\rangle$ is smaller. Thus the plots in Fig. 7 appear compressed compared to Fig. 6. It can be seen that with these four acceptors, the unacceptable ψ regions in the $\langle\kappa^2\rangle_{min}$ plots are reduced considerably, and unacceptable regions in the $\langle\kappa^2\rangle_{max}$ plots have vanished completely for both surface and volume averaging.

Transfer from One Donor to Two Acceptors/Actin Filament

Although, due to the range for FRET energy transfer, four acceptors are often assumed for the geometry of F-actin, there are situations in which the transfer does not extend to more than two nearest acceptors (subunits ± 1; Fig. 5). This will be true if the radial coordinate r_a is small (e.g., 10 Å) [8]. Figure 8 illustrates such a case with r_a equal to 10 Å and transfer occurring from subunit 0 to subunits ± 1. As might be expected, the $\langle\kappa^2\rangle_{max}$ and $\langle\kappa^2\rangle_{min}$ plots show more acceptable regions than Fig. 6 but more unacceptable regions than Fig. 7. This result is consistent with the situation of two acceptors contributing to the average of the orientation factor, rather than one or four. Additionally, at large radial coordinates the energy transfer is between the donor and the two "next-nearest" acceptors only (subunits ± 2; Fig. 5) [8]. Ex-

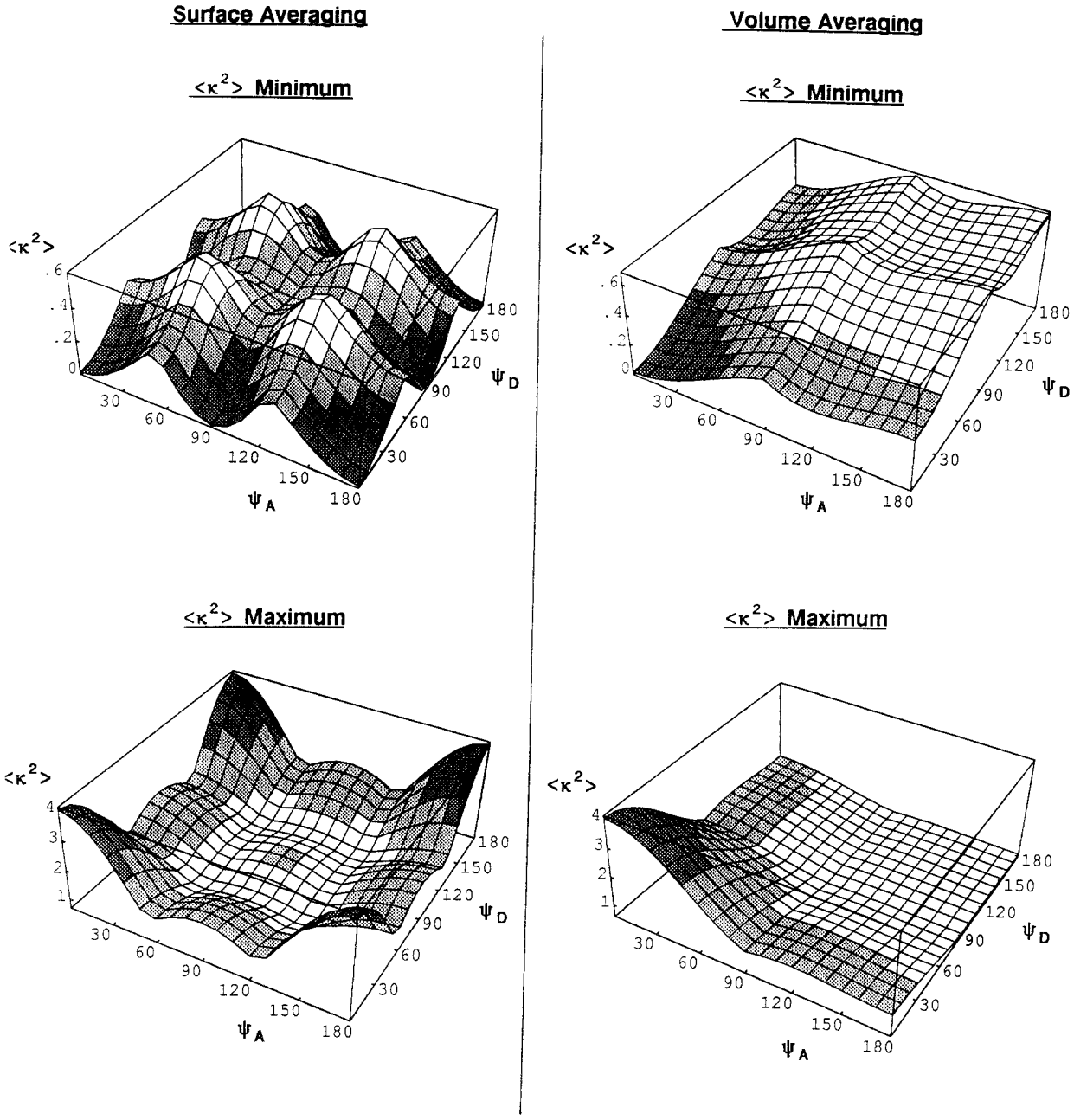

Fig. 6. Extrema plots for $\langle\kappa^2\rangle$, single donor–single acceptor. These plots represent the extreme minimum and maximum $\langle\kappa^2\rangle$ values, calculated for all cone half-angles ψ_D and ψ_A. Plots for the surface-averaged dipoles and the volume-averaged dipoles are displayed. The shading indicates the amount of error on the interprobe distance r that would result due to the application of $\langle\kappa^2\rangle = 2/3$ at those cone half-angles (see Methods).

trema plots have also been generated for radial coordinate $r_a = 40$ Å (transfer from subunit 0 to subunits ± 2) that are similar in appearance to Fig. 8. As in the situation for small radial coordinate plots, the range of $\langle\kappa^2\rangle$ in the large r_a plots is intermediate between Fig. 6 and Fig. 7 (results not shown).

As in the case at $r_a = 25$ Å, where the intermonomer distances to each of the four relevant acceptors was the same, at $r_a = 10$ Å and $r_a = 40$ Å the distance from the donor to the two relevant acceptors in each situation is the same. This allows the simple calculation of a $\langle\kappa^2\rangle$ that applies to the system.

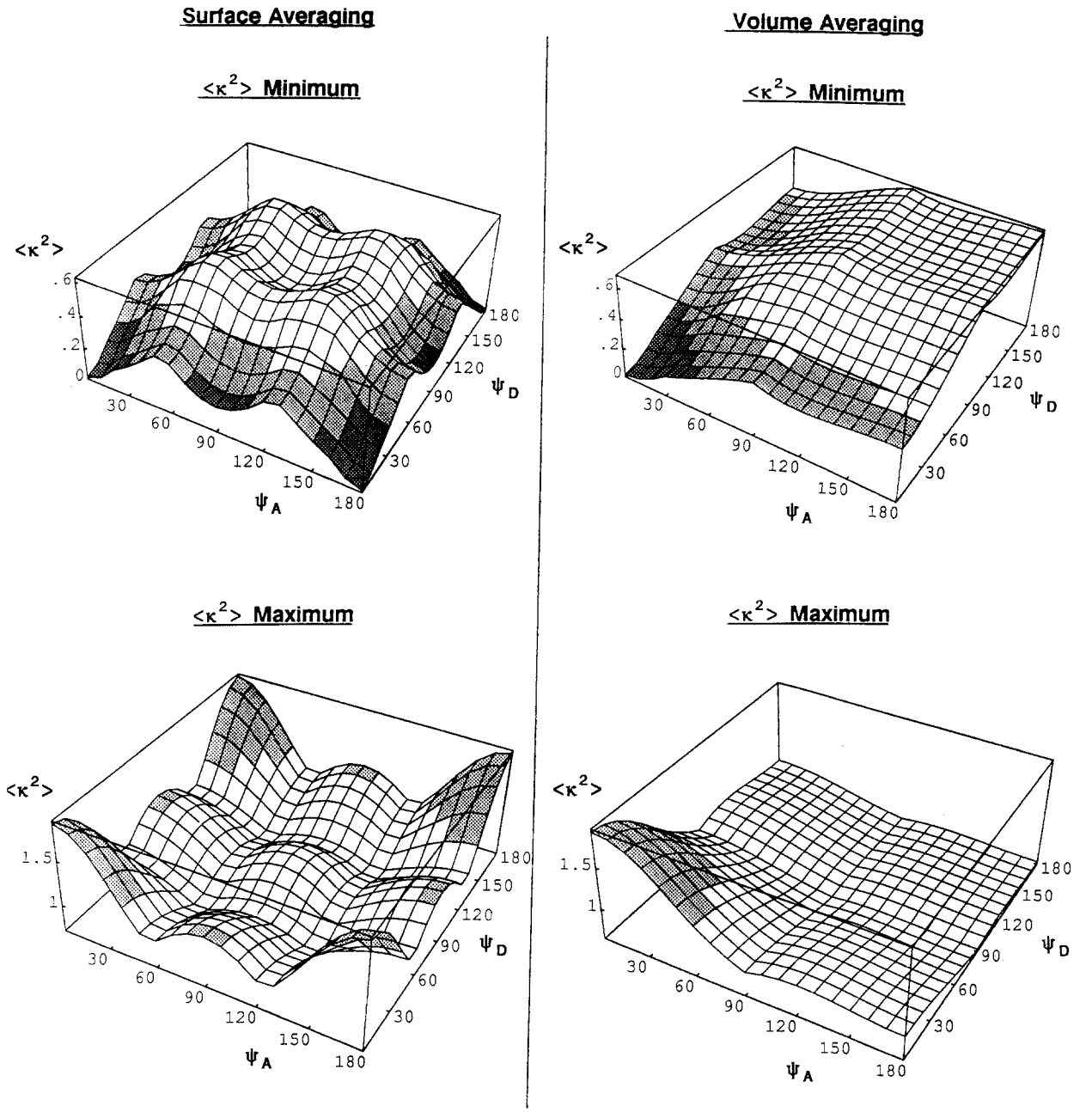

Fig. 7. Extrema plots for $\langle\kappa^2\rangle$, one donor–four acceptors/actin filament. Same as Fig. 6 except that the averaging of $\langle\kappa^2\rangle$ takes into account the simultaneous energy transfer to four acceptors which are located symmetrically on the actin filament (Fig. 5). In this case, the donors and acceptors are all located 25 Å radially from the theoretical actin filament axis.

DISCUSSION

Single Donor–Single Acceptor

In establishing the limits for $\langle\kappa^2\rangle_{max}$ and $\langle\kappa^2\rangle_{min}$ using depolarization analysis, often the best that can be accomplished is a partial solution. Depolarization analysis uses the axial depolarization factors d^x and the associated angle Θ_T [5, 10] [see also Eq. (3) and Fig. 1]. In depolarization analysis, the angle Θ_T can turn out to be two-valued, and this usually leaves the unsatisfactory

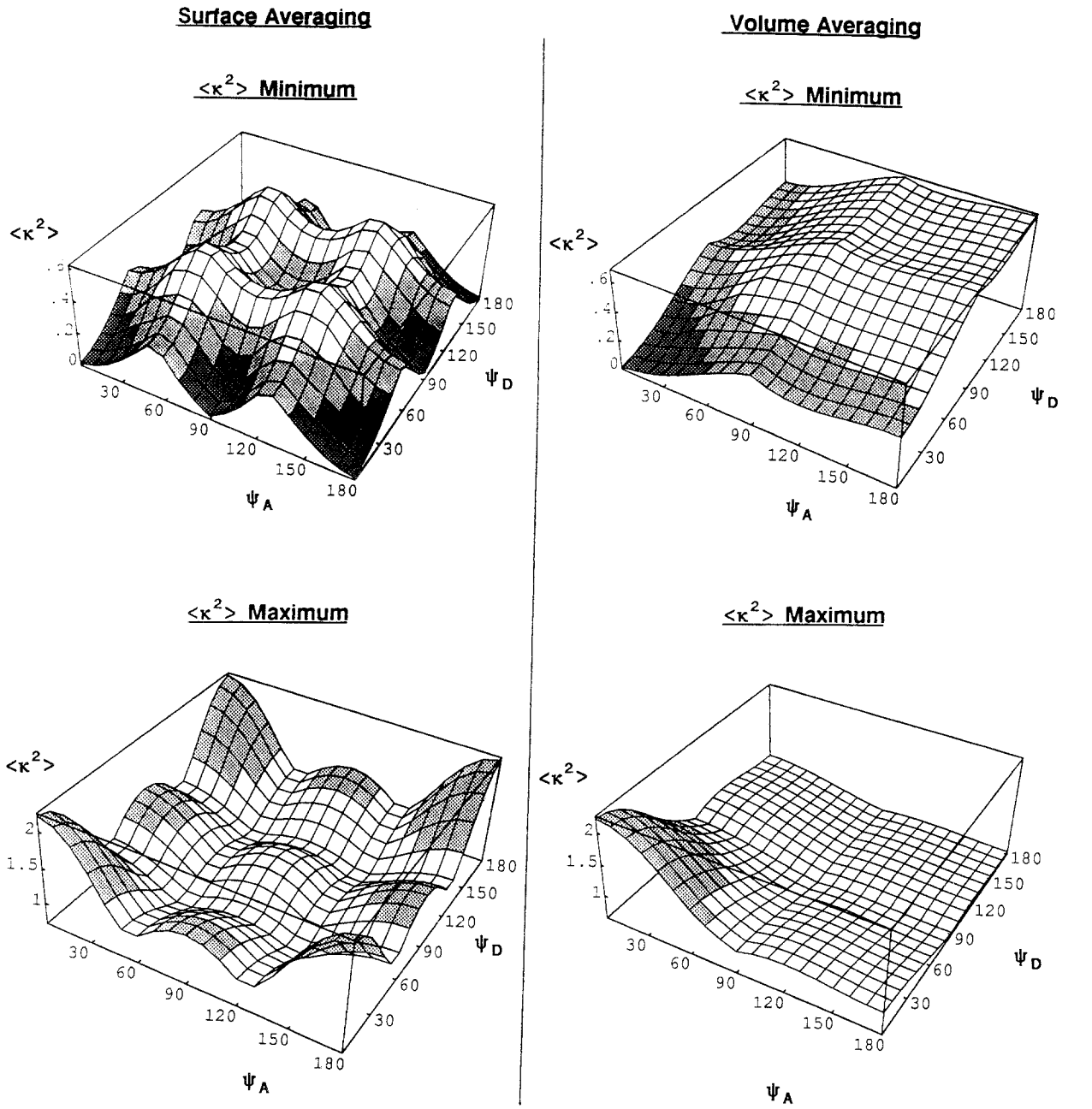

Fig. 8. Extrema plots for $\langle\kappa^2\rangle$, one donor–two acceptors/actin filament. Same as Fig. 7 except that there is concurrent energy transfer only to the two nearest acceptors (subunits ± 1; Fig. 5). The radial coordinate for the donor and acceptor chromophores in this case is 10 Å.

option of establishing maximum and minimum limits for $\langle\kappa^2\rangle$ that are valid only when both $\langle d^x_D\rangle$ and $\langle d^x_A\rangle$ are positive [5]. The restriction that this requirement (on the depolarization factors) places on the donor and acceptor cone half-angles can be seen from Fig. 4. When volume averaging applies, for a positive axial depolarization factor to occur, the cone half-angles ψ must be less than $\pi/2$. If a dipole is surface averaged, ψ cannot be between 54.7 and 125.3°. These restrictions reduce the general effectiveness of this method and can leave the applicability of $\langle\kappa^2\rangle = 2/3$ in doubt.

In contrast, the modeling of a system in terms of cone angles to establish acceptable $\langle\kappa^2\rangle_{max}$ and $\langle\kappa^2\rangle_{min}$ limits can directly provide a strategy for choosing fluo-

rophores and can more clearly demonstrate the applicability of the use of the $\langle\kappa^2\rangle = 2/3$ value. From Fig. 6 it is seen that, for single donor–single acceptors, it is best to use fluorophores that satisfy volume averaging and satisfy the condition that either the donor or the acceptor have a cone half-angle $\psi > 60°$. This condition requires that the experimental axial depolarization be less than 0.375. Figure 6 also shows that particular combinations of surface averaged donor and acceptor dipoles will also be acceptable, for instance, if both the donor and the acceptor cone half-angles are between 45 and 135°. While these specific conditions must be met for surface averaging, volume averaging has the advantage that at larger donor or acceptor cone half-angles, the use of the isotropic orientation factor becomes more acceptable.

Physically, volume averaging corresponds to the transition dipoles having more motional freedom than surface averaging. Surface averaging of the dipole movement may be a good approximation if the chromophoric moiety of a donor or acceptor is linked to a protein via a covalent bond and if the motion of the chromophore takes place in a rigid region of the protein. However, if the motion of the chromophoric moiety is influenced by fluctuations of the surrounding structure, the transition dipole could be found anywhere within the volume of a cone and not necessarily be restricted to a conical surface. Volume averaging therefore provides a model which is a more general description of the dipole movement and may be more appropriate to invoke in the absence of specific information.

Single Donor–Multiacceptor/Actin Filament

In the multiacceptor F-actin case, the use of depolarization analysis for obtaining $\langle\kappa^2\rangle$ limits would be difficult and may not yield unique information. This type of analysis would involve the appropriate deconvolution of transfer depolarization information from as many as four concurrent acceptors. However, using the cone angle method, we can apply the simple symmetry underlying F-actin to generate the spatial relationship between the donor and each acceptor as given in the Appendix. This allows a straightforward calculation of $\langle\kappa^2\rangle$.

As can be seen from the maxima plots in Fig. 7 [and also Eq. (9)], in the transfer to four acceptors, the calculated $r_{2/3}$ for F-actin will never underestimate the actual distance by more than 20% regardless of the ψ angles (and hence axial depolarization) whether surface or volume averaging applies. For volume averaging, the error in $r_{2/3}$ is considerably less for the larger ψ angles. As a matter of strategy, to ensure that $r_{2/3}$ is also within +20% of the actual distance when volume averaging applies [minima plot; Fig. (7)], it would be best to choose chromophores where either the donor or the acceptor cone half-angle exceeds 45°. This condition is satisfied if the axial depolarization of one chromophore is less than 0.6.

Experimentally, the acceptor frequently is not fluorescent and its axial depolarization factor cannot be determined. The present analysis indicates that this situation does not pose any problem in the estimate of the lower bound of the distance. The several donor and acceptor probes that have been used for actin have axial depolarization factors usually >0.6, with the value of some probes being in the range of 0.74–0.86 [8, 11], corresponding to ψ angles in the range of 40–30° (for volume averaging). Note that this same range of axial depolarization factors corresponds to ψ angles in the range of 25–18° for surface averaging. Thus there is some uncertainty in the upper bound of the donor–acceptor distance that has been determined with these probes.

F-Actin FRET and $\langle\kappa^2\rangle$

The radial coordinates r_a and intrasubunit and intersubunit distances of F-actin derived from FRET measurements provide a means to investigate the global conformation of the helical filament and the extent to which the conformation is perturbed when the filament is decorated with the muscle regulatory proteins troponin and tropomyosin. Also of interest is the effect of the interaction of actin with myosin on the actin conformation, particularly the flexibility between regions within the actin monomer [12]. These questions are being addressed in several laboratories using average distances obtained from standard FRET measurements as well as the recently developed methodologies to determine distributions of the donor–acceptor distances [13, 14]. A recognized potential problem with these studies relates to the uncertainty of the orientation factor. While evidence from other methods, including X-ray fiber diagrams [15], generally agrees very well with FRET-derived actin radial coordinates, the question of the confidence in $\langle\kappa^2\rangle = 2/3$ has been an ongoing one.

The analysis presented here represents a conservative "worst-case" approach to the problem. The values for the absolute minima and maxima of the average orientation factor are investigated rather than using values that may be considered to be statistically probable. In addition, the amount of freedom of the fluorophore is restricted by the use of a simple cone model having a single axis of rotation.

The condition of a single dipole moment for each donor and for each acceptor in our analysis is a very

cautious assumption. Haas *et al.* [4] and Steinberg [16] state that for absorption and emission characterized by two or more incoherent dipole moments, the range of the orientation factor is markedly decreased compared with corresponding cases in which the donor and acceptor are characterized by a single dipole each. Torgerson and Morales [17] put forth that the multiplicity in the acceptor absorption transition dipole reduces the uncertainty in κ^2. The results of the present F-actin FRET analysis are consistent with these views. A multiplicity in the number of acceptor fluorophores at the same distance from the donor (here up to four)—with each individual acceptor characterized by a single dipole moment—can be considered (with regard to $\langle\kappa^2\rangle$) to be mathematically analogous to a single acceptor fluorophore having multiple incoherent dipole moments. The present work has demonstrated that the range for the dynamically averaged value of the orientation factor is greatly reduced for the case of multiple acceptor fluorophores with a single dipole moment per acceptor. It is intuitively clear that multiple dipole moments for each acceptor fluorophore will further randomize the average orientation factor and will justify even more the use of the isotropic 2/3 value.

SUMMARY

In order to have maximum usefulness in obtaining molecular distances using FRET techniques, chromophores must be chosen so that $\langle\kappa^2\rangle = 2/3$ may be generally applied without requiring knowledge of the mean donor and acceptor orientations. A worst-case analysis shows that with dipole volume averaging and a single donor–single acceptor situation, it is best to use a donor–acceptor pair one of which has a cone half-angle of at least 60°. For energy transfer occurring across the monomeric subunits of F-actin, intermolecular distances are not underestimated by more than 20%, and it is unlikely that they are overestimated by this amount. Due to the multiplicity of acceptors in F-actin FRET experiments, less motion is required of the chromophores in order to apply $\langle\kappa^2\rangle = 2/3$. Because of the strict assumptions made in this analysis we feel that the use of $\langle\kappa^2\rangle = 2/3$ in F-actin radial coordinate studies is clearly warranted.

APPENDIX: Calculation of $\langle\kappa^2\rangle$ Using Dipole Symmetry Relationships in F-Actin

Single–Donor/Single–Acceptor $\langle\kappa^2\rangle$ Calculation

It can be seen directly from Figs. 1 and 2 and Eqs. (5)–(8), (10), and (11) that $\langle\kappa^2\rangle$ can be calculated for any given cone half-angles ψ_D and ψ_A. After surface or volume averaging has been chosen for these cone half-angles [Eq. (10) or (11)], then all possible mean orientation angles (Θ_D, Θ_A, Φ) must be tested [Eqs. (5) and (6)]. Using the computer, each of these angles (which represent the relative orientations of the theoretical central cone vectors) is independently varied. Every combination (Θ_D, Θ_A, Φ) will yield a value for $\langle\kappa^2\rangle$. The maximum and minimum values for $\langle\kappa^2\rangle$ for an entire set of (Θ_D, Θ_A, ϕ) establish the limits on the orientation factor for one given ψ_D and ψ_A pair. The whole process is then repeated, independently stepping through all ψ_D and ψ_A between 0 and π in order to produce the three-dimensional extrema plots for $\langle\kappa^2\rangle$, such as those shown in Fig. 6.

Note that in the single-donor/single-acceptor case, κ^{x2} must be calculated using Eq. (6) [which is related to Eq. (4)], rather than using a form of Eq. (3). Equation (3) involves the dot product of three vectors, however, the individual angles (θ_T, θ_D, θ_A) are not independent variables. This can be seen from the fact that if $\theta_D = \theta_A = 0°$, then it is impossible for θ_T to be nonzero (Fig. 1). Thus a computer program that checks all possible central cone vector orientations cannot simply loop through all θ_T, θ_D, and θ_A in an unconstrained manner. This is not to say that the three dot products in Eq. (3) are incorrect for specifically compatible angles θ_T, θ_D, and θ_A. However, care must be taken to ensure that for any general orientation, the dot products are expressed in terms of fully independent variables (see sections below).

$\langle\kappa^2\rangle$ Calculation for F-Actin

To calculate $\langle\kappa^2\rangle$ for the single-donor/four-acceptor case in F-actin, we must first calculate $\langle\kappa^2\rangle$ between the donor and each acceptor separately, then obtain the average orientation factor for the single-donor/four-acceptor system. In this situation, we first calculate $\langle\kappa^2\rangle_{+1}$, between the donor D and the acceptor A_{+1}, on monomer $+1$ (Fig. 5). This is carried out for particular cone half-angles ψ_D and ψ_{A+1}. We can note immediately that all acceptor cone half-angles are identical, $\psi_{A+1} = \psi_{A+2} = \psi_{A-1} = \psi_{A-2}$. We also realize that, due to F-actin helical symmetry, after specifying a mean spatial orientation for the dipole that is associated with A_{+1}, we can generate the exact spatial orientations for the mean positions A_{+2}, A_{-1}, and A_{-2}. Therefore, we can average $\langle\kappa^2\rangle_{+1}$, $\langle\kappa^2\rangle_{+2}$, $\langle\kappa^2\rangle_{-1}$, and $\langle\kappa^2\rangle_{+2}$ to produce an overall $\langle\kappa^2\rangle$ for the single-donor/four-acceptor system.

Independent spatial variables based on F-actin symmetry can be used to describe donor and acceptor dipole

orientations. This allows the axial orientation factor κ^{x2} to be calculated using the dot product of three vectors. Following Eq. (3), we can write

$$\kappa^{x2}_j = [(\mathbf{D}\cdot\mathbf{A}_j) - 3(\mathbf{D}\cdot\mathbf{V}_j)(\mathbf{A}_j\cdot\mathbf{V}_j)]^2 \qquad \text{(A1)}$$

Here boldface type denotes unit vectors and the index j refers to a particular monomer, either $+1$, $+2$, -1, or -2. Thus, **D** is the unit vector representing the theoretical central vector for the mobile dipole attached to monomer 0, $\boldsymbol{A}_j$ represents the unit vector for the theoretical central vector for the mobile acceptor dipole attached to monomer j. $\mathbf{V}_j$ is the unit vector which starts from the residue where the donor is attached and points to the residue where the j^{th} acceptor is attached (Fig. 5). All four acceptor chromophores and the donor chromophore are attached to chemically equivalent residues in each respective monomer. All acceptors are attached to the subunits in an identical manner, and the mean orientations of the attached acceptors are simply rotated and translated according to F-actin helical symmetry. However, the mean orientation of the donor is independent, as it is assumed to be a different chromophore than the acceptors.

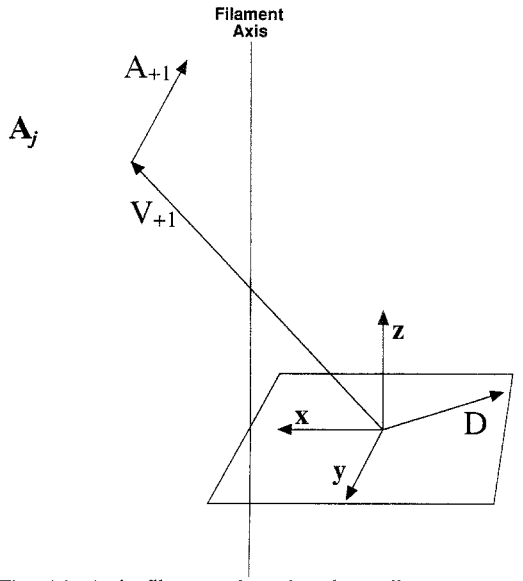

Fig. A1. Actin filament, donor-based coordinate system. Mutually orthogonal **x,y,z** axes are centered on the residue to which the donor is attached. Detailed description in text. (All donor and acceptor vectors shown in Figs. A1–A6 can be considered to be either dipoles of cone half-angle 0°, or the axis of symmetry of the individual dipole distributions.)

Donor-Centered Coordinate Systems

Consider a donor-based coordinate system (**x, y, z**) whose origin (0, 0, 0) is the residue on which the donor is attached (Fig. A1). In this system, **z** points directly up, parallel to the actin filament axis. The **x–y** plane is perpendicular to the filament axis, with **x** pointing from the donor-attached residue directly toward the filament axis and **y** pointing directly out of the paper (as shown). It should be noted that this is a right-handed (counterclockwise) coordinate system and that the actin helix is characterized by a (left-handed) rotation of $\theta_h = -166°$ between adjacent monomers [18]. The projected distance z_h, along the **z** axis and between chemically equivalent residues on adjacent monomers, is determined by the actin helical parameters and is equal to 27.5 Å. The distance along the **x** axis from the origin to the filament axis is simply the radial coordinate r_a.

We can define an angle θ from the projection of a vector onto the **x–y** plane. This azimuthal angle is in the **x–y** plane and increases counter-clockwise from 0 to 2π (Fig. A2). We also define a polar angle ϕ, between a vector and the filament axis. This angle increases from the positive **z** axis from 0 to π (Fig. A3). Thus, the donor central vector **D**, the four acceptor central vectors $\mathbf{A}_j$, and the four position vectors $\mathbf{V}_j$ (between donor and acceptors) can all be written in terms of θ and ϕ angles. In general,

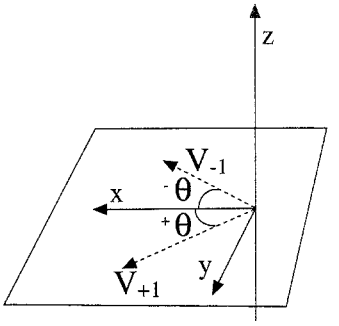

Fig. A2. Azimuthal angle. This is the θ angle made from the projection of a vector onto the **x–y** plane with **x** axis.

$$\mathbf{p} = (\sin\phi_p\cos\theta_p)\mathbf{x} + (\sin\phi_p\sin\theta_p)\mathbf{y} + (\cos\phi_p)\mathbf{z} \qquad \text{(A2)}$$

The symbol p can stand for either D, A_{+1}, A_{+2}, A_{-1}, A_{-2}, V_{+1}, V_{+2}, V_{-1}, or V_{-2}. For example,

$$\mathbf{D} = (\sin\phi_D\cos\theta_D)\mathbf{x} + (\sin\phi_D\sin\theta_D)\mathbf{y} + (\cos\phi_D)\mathbf{z}$$

$$\mathbf{A}_{+2} = (\sin\phi_{A+2}\cos\theta_{A+2})\mathbf{x} + (\sin\phi_{A+2}\sin\theta_{A+2})\mathbf{y} + (\cos\phi_{A+2})\mathbf{z}$$

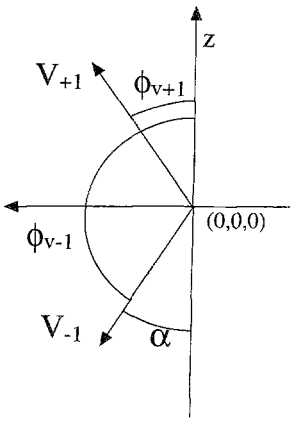

Fig. A3. Polar angle. This is the ϕ angle made between a vector and the z axis ($\mathbf{V}_{+1}$, $\mathbf{V}_{-1}$ shown here).

The dot product of these two vectors is

$$\begin{aligned}\mathbf{D} \cdot \mathbf{A}_{+2} = &(\sin \phi_D \cos \theta_D \sin \phi_{A+2} \cos \theta_{A+2}) \\ &+ (\sin \phi_D \sin \theta_D \sin \phi_{A+2} \sin \theta_{A+2}) \\ &+ (\cos \phi_D \cos \phi_{A+2})\end{aligned}$$

In this way, all the dot products between vectors may be calculated in Eq. (A1) for each monomer j.

Symmetry Relationships Between Acceptor Dipoles and Position Vectors

In order to simplify the application of Eqs. (A1) and (A2) in the calculation of κ^{x2} for F-actin, we first need to determine the following expressions

ϕ_{A+n} in terms of ϕ_{A+1}
θ_{A+n} in terms of θ_{A+1}, θ_h
ϕ_{V+j} in terms of r_a, θ_h, z_h
θ_{V+j} in terms of θ_h

where $n = +2, -1$, or -2, and $j = +1, +2, -1, -2$.

By formulating the problem in this way, we can calculate κ^{x2} for the multiacceptor F-actin system using only two angular variables (ϕ_{A+1}, θ_{A+1}) to define all four acceptors mean orientations. To specify this energy transfer system completely, we also need two independent angular variables for the donor (ϕ_D, θ_D), along with the constants r_a, θ_h, and z_h. [Note that the radial coordinate (r_a) value is assumed to be the same for all labeled chromophores.] The other parameters listed above, θ_h and z_h, were defined previously and are established by the F-actin symmetry.

The most direct relationship to determine is the one between the acceptor ϕ angles. Consider a vertical axis, parallel to the z and filament axes, drawn through each acceptor residue at the point of attachment. It is clear that each acceptor central vector will make the same angle ϕ with the vertical axis. Thus for any given ϕ_{A+1} we have

$$\phi_{A+1} = \phi_{A+2} = \phi_{A-1} = \phi_{A-2} \qquad \text{(A3)}$$

Next we obtain the relationships between the acceptor θ angles. For this we project the four acceptor dipoles on the **x–y** plane, as in Fig. A4. The left-handed rotation of 166° (i.e., $\theta_h = -166°$) between successive monomers is the same as a $360 - 166 = 194°$ right-handed rotation. We see that for the relationship between acceptor dipoles on successive monomers, the amount of monomer rotation is simply carried through to the acceptor dipoles. Therefore, it follows that for a given θ_{A+1},

$$\begin{aligned}\theta_{A+2} &= \theta_{A+1} + \theta_h = \theta_{A+1} - 166° \\ \theta_{A-1} &= \theta_{A+1} - 2(\theta_h) = \theta_{A+1} + 332° \\ \theta_{A-2} &= \theta_{A+1} - 3(\theta_h) = \theta_{A+1} + 138° \end{aligned} \qquad \text{(A4)}$$

(The acceptor subunit A_{-1} is two monomers away from acceptor A_{+1}, since the donor subunit intervenes.)

For the intermonomer position vectors **V** (from the donor residue to each acceptor residue), we can obtain the following relationships for θ angles. The projection in Fig. A2 demonstrates that in the donor-centered coordinate system, vector $\mathbf{V}_{+1}$ is simply reflected across the x axis from vector $\mathbf{V}_{-1}$, and likewise $\mathbf{V}_{+2}$ is reflected across the x axis from $\mathbf{V}_{-2}$. This means that $\theta_{v-1} = -\theta_{v+1}$, and $\theta_{v-2} = -\theta_{v-2}$.

Figure A5 shows the geometry for θ_{v+1}, θ_{v+2}. Keeping in mind the direction of positive rotation in the donor-centered **x–y** plane, we have $\theta_{v+1} = 0.5\,(180 - 166) = 7°$ and $\theta_{v+2} = 0.5\,(180 - [360 - 2(166)]) = -76°$. Thus

$$\theta_{v+1} = 7°$$

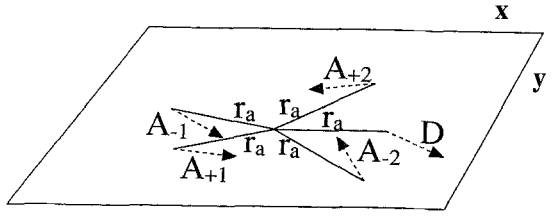

Fig. A4. Rotational symmetry between acceptors. The rotational relationship between acceptor vectors $\mathbf{A}_{+1}$, $\mathbf{A}_{+2}$, $\mathbf{A}_{-1}$, and $\mathbf{A}_{-2}$, which are attached to helically related monomers, as seen in projection onto the **x–y** plane.

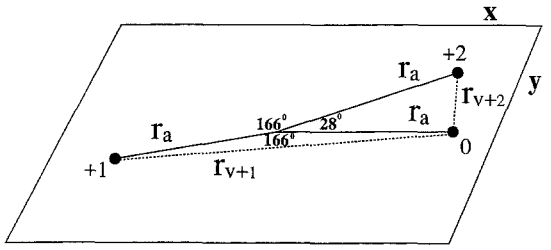

Fig. A5. Projected lengths of **V** vectors. The distances r_{v+1} and r_{v+2} represent the projected lengths of the $\mathbf{V}_{+1}$ and $\mathbf{V}_{+2}$ vectors onto the **x–y** plane.

$$\begin{aligned}\theta_{v+2} &= -76° \\ \theta_{v-1} &= -7° \\ \theta_{v-2} &= 76°\end{aligned} \qquad \text{(A5)}$$

For the ϕ_v angles, we can look at Fig. A3 and consider the $\mathbf{V}_{+1}$ and $\mathbf{V}_{-1}$ vectors to be rotated around the **z** axis so that they lie in the **x–z** plane, and their respective ϕ angles with the **z** axis are preserved. By symmetry, the angle $\phi_{v-1} = 180 - \alpha$, and $\alpha = \phi_{v+1}$. A similar application of symmetry can be used for ϕ_{v-2}. This yields

$$\begin{aligned}\phi_{v-1} &= 180 - \phi_{v+1} \\ \phi_{v-2} &= 180 - \phi_{v+2}\end{aligned} \qquad \text{(A6)}$$

To get ϕ_{v+1} and ϕ_{v+2}, we first consider Fig. A5 and the distances r_{v+1} and r_{v+2}. These distances represent the projected lengths of the associated vectors $\mathbf{V}_{+1}$ and $\mathbf{V}_{+2}$ onto the **x–y** plane. Since we know that the radial distance to the filament axis is the same for all labeled residues and that the angular rotation between chemically equivalent points on successive monomers is 166°, then we have these simple relationships:

$$\begin{aligned}(r_{v+1})^2 &= (r_a)^2 + (r_a)^2 - 2(r_a)^2 \cos(166°) \\ (r_{v+2})^2 &= (r_a)^2 + (r_a)^2 - 2(r_a)^2 \cos(28°)\end{aligned}$$

or

$$\begin{aligned}(r_{v+1}) &= r_a\sqrt{2}[1 - \cos(166°)]^{1/2} \\ (r_{v+2}) &= r_a\sqrt{2}[1 - \cos(28°)]^{1/2}\end{aligned} \qquad \text{(A7)}$$

Next we consider a plane that includes the **z** axis (i.e., the axis associated with the donor residue, rather than the filament axis), the intermonomer position vector $\mathbf{V}_{+1}$, and the projected distance r_{v+1} (Fig. A6a). A similar plane can be drawn for the respective +2 vectors (Fig. A6b). Using the fact that the projected *z* distance from the donor to monomer +2 is $2z_h$, we obtain the following for angles ϕ_{v+1} and ϕ_{v+2}:

$$\phi_{v+1} = \tan^{-1}(r_{v+1}/z_h)$$

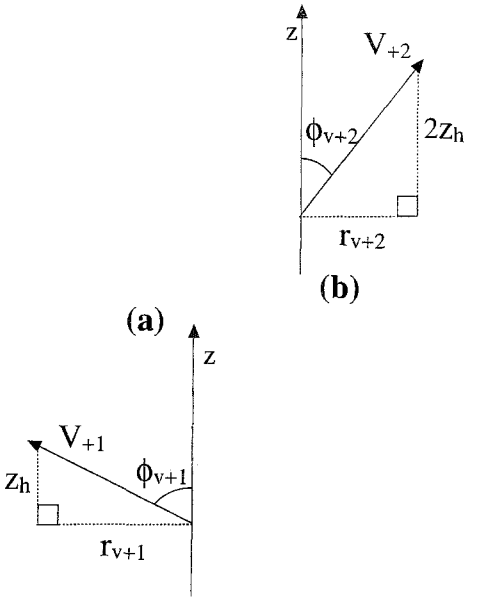

Fig. A6. Polar angle for **V** vectors. The geometry for obtaining the ϕ angles for the **V** vectors. The projected lengths r_v are the same as shown in Fig. A5. (a) The polar angle for the $\mathbf{V}_{+1}$ vector. (b) The polar angle for the $\mathbf{V}_{+2}$ vector.

$$\phi_{v+2} = \tan^{-1}(r_{v+2}/2z_h) \qquad \text{(A8)}$$

Equations (A6)–(A8) completely define the ϕ angles for the **V** vectors.

ACKNOWLEDGMENTS

This work was supported in part by Grants AR25193 and AR31239 from the National Institutes of Health (H.C.C.). We acknowledge computer time provided by the Department of Physics, University of Alabama at Birmingham.

REFERENCES

1. H. C. Cheung (1981) in J. R. Lakowicz (Ed.), *Topics in fluorescence Spectroscopy. Vol. 2: Principles*, Plenum Press, New York, pp. 127–176.
2. T. Förster (1948) *Ann. Phys. (Leipzig)* **2,** 55–77.
3. Z. Hillel and C.-W. Wu (1976) *Biochemistry* **15,** 2105–2113.
4. E. Haas, E. Katchalski-Katzir, and I. Z. Steinberg (1978) *Biochemistry* **17,** 5064–5070.
5. R. E. Dale, J. Eisinger, and W. E. Blumberg (1979) *Biophys. J.* **26,** 161–194.
6. D. L. Taylor, J. Reidler, J. A. Spudich, and L. Stryer (1981) *J. Cell Biol.* **89,** 362–367.

7. M. Miki, J. A. Barden, and C. G. dos Remedios (1986) *Biochim. Biophys. Acta* **872,** 76–82.
8. A. A. Kasprzak, R. Takashi, and M. F. Morales (1988) *Biochemistry* **27,** 4512–4522.
9. R. E. Dale and J. Eisinger (1974) *Biopolymers* **13,** 1573–1605.
10. R. E. Dale and J. Eisinger (1975) in R. F. Chen and H. Edelhoch (Eds.), *Concepts in Biochemical Fluorescence, Vol. 1,* Marcel Dekker, New York, pp. 115–284.
11. H. C. Cheung and B.-M Liu (1984) *J. Muscle Res. Cell Motil.* **5,** 65–80.
12. M. Miki (1991) *Biochemistry* **30,** 10878–10884.
13. I. Gryczynsky, W. Wiczk, M. L. Johnson, H. C. Cheung, C.-K. Wang, and J. R. Lakowicz (1988) *Biophys. J.* **54,** 577–586.
14. H. C. Cheung, C.-K. Wang, I. Gryczynsky, W. Wieslaw, G. Laczko, M. L. Johnson, and J. R. Lakowicz (1991) *Biochemistry* **30,** 5238–5247.
15. K. C. Holmes, D. Popp, W. Gebhard, and W. Kabsch (1990) *Nature* **347,** 44–49.
16. I. Z. Steinberg (1975) in R. F. Chen and H. Edelhoch (Eds.), *Concepts in Biochemical Fluorescence, Vol. 1,* Marcel Dekker, New York, pp. 79–114.
17. P. M. Torgerson and M. F. Morales (1984) *Proc. Natl. Acad. Sci. USA* **81,** 3723–3727.
18. J. Squire (1981) in *The Structural Basis of Muscular Contraction,* Plenum, New York, pp. 157–179.